Some Observations on the Structure and Function of the Spinning Apparatus in the Silkworm *Bombyx mori*

Tetsuo Asakura,*,† Kosuke Umemura,† Yasumoto Nakazawa,† Haruko Hirose,‡ James Higham,§ and David Knight*,§

Department of Biotechnology, Tokyo University of Agriculture and Technology, Koganei, Tokyo 184-8588, and Material Analysis Research Laboratories, Teijin Ltd., Hino, Tokyo 191-8512, Japan, and Department of Zoology, University of Oxford, South Parks Roads, Oxford OX1 3PS, United Kingdom

Received September 15, 2006

Silkworm silk has outstanding mechanical properties despite being spun at room temperature and from aqueous solution. Although it has been proposed that fiber formation is mainly induced by shearing and extensional flow in the spinneret, the detailed structure and function of the spinning apparatus of *Bombyx mori* silkworms are still not fully elucidated. In this paper we describe three aspects of the functional microanatomy of the spinning apparatus: changes in the diameter of the silk gland duct with distance along the duct, how the birefringence of the fibroin changes as it flows down the duct, and the detailed three-dimensional structure of the silk press and related structures. The existence of a double escaped nematic liquid crystal texture in the fibroin in a region of the duct is described. After this region the birefringence suddenly disappeared until the start of an internal draw down taper which commenced just before the silk press. In the internal draw down taper the birefringence increased dramatically to an asymptotic value as a thread was drawn from the fibroin gel. The structure of the silk press suggests that it acts as a restriction die whose diameter can be regulated.

Introduction

Bombyx mori silk fibroin fibers are produced by silkworms at room temperature and from an aqueous solution, but they exhibit exceptional strength, toughness, and resistance to mechanical compression.[1,2] Silk fibroin also possesses impressive biological properties, giving it considerable potential as a biomaterial for tissue engineering.[3] Consequently, much attention has been focused on the natural mechanism of fiber formation with the aim of understanding how tough fibers are produced naturally and how the process might be mimicked industrially.

The *B. mori* raw (undegummed) silk filament (bave) emerging from the silkworm consists of two fibroin protein monofilaments (brins) enveloped in a proteinaceous sericin coat. The latter serves as an adhesive to stick the baves together in the cocoon. The fibroin brins are largely constructed from two proteins, heavy- and light-chain fibroin, linked together by disulfide bonds. The sericin coat is constructed from several different sericins, all of which are thought to be expression products of the sericin-1 and sericin-2 genes. Both the fibroin and sericin proteins are produced by two rows of very large flattened cells that make up the lining of a pair of long tubular silk glands homologous with the salivary glands of other insect larvae. Each silk gland has its own elongated duct, the silk gland duct (also referred to as the anterior division of the silk gland).[4−6] The end of the anterior portion of the secretory part of the silk gland and the start of the duct are defined by an abrupt reduction in external diameter and abrupt appearance of a cuticle lining to the lumen. The cuticle lining of the duct is surrounded by a type of epithelial cell different from that of the gland proper, containing a vesicular proton pump thought to be responsible for acidification of the contents of the lumen of the duct before spinning.[7] The ion pumping of these cells may be responsible for other changes in water and ion content along the length of the silk duct.[8−10] The silk gland duct opens into a short common duct which passes through a structure known as the silk press before running a short distance to open on a single large spigot from which the silk bave is discharged.[4−6] The spigot is mounted on the base of the labium just posterior to the mouth.[11] As shown in Figure 1, the silk protein synthesizing part of the silk gland consists of three distinct successive parts: the thin and flexuous posterior part (1), the wider middle (2), and the anterior part (3). Only the posterior part of the silk gland synthesizes the heavy- and light-chain fibroins, the main components of silk proteins, and an accessory protein, P25, thought to be concerned with fibroin assembly and intracellular transport.[12−14] Fibroin is then transported down the lumen into the middle part of the silk gland in which it is stored in a concentrated state as a weak gel until required for spinning. There is a gradient of expression of the sericin-1 gene starting at a low level in the middle part of the gland and reaching its greatest expression in the anterior part,[15] reflecting the progressive accumulation of sericin around the fibroin core.[16] Several sericins with different molecular weights are produced in these regions by differential splicing of the eight introns of the sericin-1 gene.[17] Recently, the ultrastructure of the silk glands, silk press, and spinneret of the third, fourth, and fifth instars of the noctuid moth *Helicoverpa armigera* have been described using several microscopical techniques.[18] This pest, the cotton bollworm, is not closely related to the silkworms but produces a silk which plays a role in feeding, dispersal, formation of the pupation chamber, and attachment of the larva to the substrate. The structure of the

* To whom correspondence should be addressed. (T.A.) Phone and fax: +81-42-383-7733. E-mail: asakura@cc.tuat.ac.jp. (D.K.) E-mail: david.knight77@ntlworld.com.

† Tokyo University of Agriculture and Technology.

‡ Teijin Ltd.

§ University of Oxford.

10.1021/bm060874z CCC: $37.00
Published on Web 11/29/2006

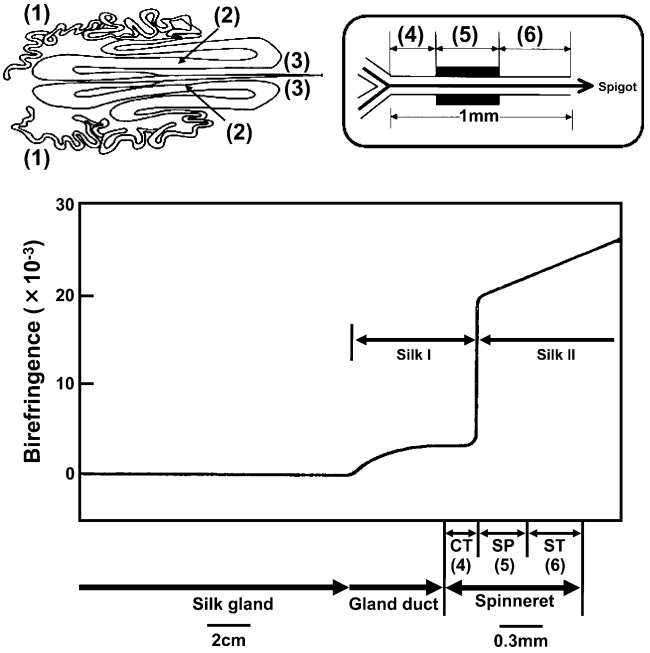

Figure 1. Structure and function of the silk gland, gland duct, and spinneret after Kataoka.[16,21] The silk gland (upper left) consists of a narrow diverging convoluted posterior secretory part (1), a wider S-shaped middle secretory part (2), and a narrow duct (3). The spinneret (upper right) also consists of three parts, a common tube (4), a silk press (5), and a spinning tube (6). The graph from Kataoka[16] shows how the birefringence changes in the duct and silk press.

silk press in this noctuid is clearly closely related to that of the same structure in *B. mori* described below.

The mechanism of fiber formation in the *B. mori* silkworm is, however, still not fully elucidated. The silk thread is actively pulled from the spigot by the side-to-side movement of the silkworm's head, producing a figure eight pattern.[4−6] Ogiwara[19] outlined the importance of the role of the silk press in the process of fiber formation from silk fibroin. Kataoka et al.[16,20,21] studied changes in viscosity, birefringence, and wide-angle X-ray scattering in situ at different points in the secretory pathway. Critical strain rates for the conversion of the native silk fibroin to the silk II state were estimated by forcing the silk to flow in a channel between two parallel plates under pressure.[16] The profiles of the diameter changes along the duct, viscosity of fibroin, and calculated linear velocity as it flowed through the duct during spinning were used to calculate the strain rates in the fibroin at different points along the secretory pathway.[16,20] Katoaka et al.[21] also reported that the birefringence of the nascent silk brin increased markedly in the anterior division when the silk bave was drawn artificially from the spigot at 2 cm s^{-1}. In contrast, at lower spinning speeds (0.5−1 cm s^{-1}) the increase in birefringence occurred in the lumen between the stiff plates of the silk press. The position of onset of the marked increase in birefringence varied with the spinning conditions and was said to correlate with the point in the secretory pathway at which these authors claim to have calculated that the fibroin solution reached the critical shear rate required for conversion of the silk fibroin to the β-sheet (silk II) state, although their papers do not include the primary data or detailed consideration of the assumptions they used to calculate this.[16,21] Recently, we proposed structural models for silk I (the structure of *B. mori* silk fibroin before spinning) and silk II (the structure after spinning) in the model peptide $(Ala\text{-}Gly)_{15}$ of *B. mori* silk fibroin using mainly solid-state NMR methods.[22−25] Molecular dynamics (MD) calculation was performed to simulate the structural change from silk I to silk II in poly(Ala-Gly) and to clarify the mechanism of the silk fiber formation.[26] This showed that the silk I structure (repeated type II β-turns) changes to a heterogeneous mainly antiparallel β-sheet silk II structure as a result of two factors: the removal of water molecules around the silk chains and the application of shear and stretching.

In the present study, we describe three new aspects of the functional anatomy of the mulberry silkworm's silk spinning apparatus: (i) geometry of the silk duct, (ii) changes in the birefringence of the fibroin with distance along the duct, and (iii) detailed structure of the silk press. Our results lead to an extension and reinterpretation of the process of natural silk spinning in *B. mori* and highlight a remarkable similarity to the way in which silkworms and orb web spiders spin their silk.

Experimental Section

Three-Dimensional Reconstruction. *B. mori* larval silkworms were reared on an artificial diet in our laboratory. For serial sectioning, the silk press of a fifth (final) *B. mori* larval instar that had just started to spin (at a rate of approximately 1 cm s^{-1} [19]) was fixed in situ without prior anaesthesia by irrigation with a solution containing a final concentration of 5% glutaralaldehyde and 0.1 M sodium cacodylate/HCl buffer. The silk press was dissected out in this solution and left for 6 days at 4 °C before postfixation in aqueous 1% osmium tetroxide for 1 day[27] after being washed in 0.1 M phosphate buffer. After the silk press was embedded in Epon, 1 μm serial sections were cut on an ultramicrotome with a diamond knife and stained with aqueous 1% toluidine blue in borax before examination and photomicrography with a light microscope (10× objective). The three-dimensional architecture was reconstructed using the software TRI/3D-VOL (RATOC System Engineering Co. Ltd., Tokyo). The reconstruction was prepared by tracing the outlines of the lumen, the stiff plates within the silk press, and nascent (incompletely formed) fibroin brins on the computer after the images were brought into registration.[19]

Observation of Whole Mounts. Naturally spinning *B. mori* larvae as above were rapidly opened by a longitudinal dorsal incision and the abdominal contents, fixed in situ by gentle infusion (30 min at 4 °C) followed by immersion (3 h at 4 °C) in a modified Karnovsky fixative. The fixative contained final concentrations of 2% glutaraldehyde, 2% freshly depolymerized formaldehyde, 0.1 M sodium cacodylate, 0.01 M calcium chloride, and 0.1 M sodium chloride and was adjusted to pH 7.4 with hydrochloric acid. The fixative was designed to avoid artefactual swelling or shrinkage of the silk fibroin in situ, by keeping the osmotic potential, predicted from data presented by Maser et al.,[28] only slightly in excess (475 mOsm) of that of lepidopteran hemeolymph and Ringer solutions (300−400 mOsm). A glutaraldehyde fixative was chosen for the following reasons. Dilute solutions of glutaraldehyde are widely used in immunocytochemistry because they are able to preserve the structure of the epitope in a wide range of globular and fibrous proteins, e.g.,[29,30] suggesting that they are capable of preserving much of the tertiary structure of proteins. In addition there is evidence that glutaraldehyde fixation is able to preserve a range of different lyotropic liquid crystal phases and complex patterns of molecular orientation in liquid crystalline structural proteins including mantis oothecal protein, collagens, and spider fibroin.[31−33] The silk bave was carefully cut approximately 5 mm from the spigot to avoid any stretching of the nascent brin during subsequent processing. Thereafter the silk glands were dissected out in the fixative buffer and gradually dehydrated in progressively higher concentrations of Farrant's gum before preparation of whole mounts in the fully concentrated gum, taking care not to strain any part of the preparation. A Vickers polarizing microscope fitted with a first-order red compensator was used to investigate the birefringence in whole mounts of the entire length of the duct. The polarizing microscope was equipped with a rotating analyzer, $\lambda/4$ compensator, monochromatic green filter (λ = 546 nm),

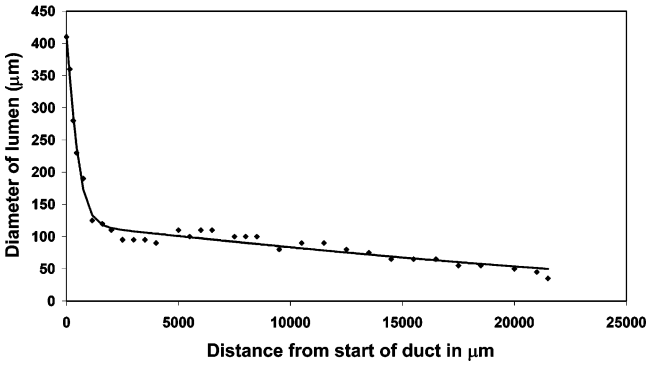

Figure 2. Graph showing the decrease in diameter of the lumen of the duct with distance from the point of commencement of the cuticle lining. A best fit second-order exponential regression line is shown, regression line $Y = A(1/(1 + \exp(BX)) + C(1/(1 + \exp(DX))$, where $A = 238$, $B = 6.18\text{E}{-}05$, $C = 588$, $D = 0.003$, and $R^2 = 0.988$.

and 40× objective to determine specific retardation of nascent brins at different distances along the duct using the quarter wave plate method.[34] The distance along the duct from the start of the draw down taper and thickness of the nascent brin at each distance were measured with a calibrated eyepiece graticule. The specific retardation was expressed in arbitrary units as no method was available for accurately determining the retardation of the compensator at the wavelength used. To determine the diameter of the lumen at different locations along the silk gland duct, whole mounts were prepared as above but with supported coverslips to prevent compression. Diameter measurements were made directly on a montage of digital photomicrographs showing the entire length of the duct.

Results and Discussion

Profile of the Silk Gland Duct. Figure 2 shows the change in diameter of the lumen of the silk gland duct with distance from its start. The diameter of the lumen showed a rapid initial decline and then fell more slowly. A second-order exponential decay fitted the data well ($R^2 = 0.988$). Thus, the convergence and size of the duct approximate those of the major ampullate silk gland duct in the orb web spider *Nephila edulis*.[35] The progressive narrowing of the silkworm's duct, as in the spider's, may, by maintaining a low and fairly constant extensional flow, help to prevent premature silk II formation as the fibroin flows through the duct during spinning. In addition, the silkworm's duct like the spider's is thought to create pH and metallic cation gradients to increase the sensitivity of the fibroin to shear.[8,9,36] Thus, the initial, rapidly converging part of the duct would, as in the spider,[10] provide for a slow linear movement of the fibroin solution along the duct and hence give a long time for treating the fibroin with ions in this part of the duct.

Birefringence Changes in the Fibroin at Different Distances along the Silk Gland Duct. At the start of the duct the fibroin in the lumen showed a pattern of isogyres (dark lines between crossed polaroids) (not shown) similar to that seen in the analogous region of the spider's duct,[35] suggesting the existence of a simple escaped nematic liquid crystal texture. Further along the duct, where the diameter had reached about 80 μm, the fibroin in many of the silk ducts studied showed (Figure 3) a more complex pattern closely similar to that seen in the analogous part of the spider's duct.[35] This was identified as the cellular optical texture, a bidirectionally escaped nematic texture first described in a synthetic amphiphile confined to a small tube.[37] The close similarity of this texture in the silkworm and spider and the observation that both appear where the lumen has constricted to approximately the same size in both organisms suggest that the fibroin solution at this location in both organisms is present as a nematic discotic (N_D) phase and that the ratios between the bend and splay Ericksen coefficients of the two fibroins are closely similar.[37]

Further down the duct, where the diameter had fallen to about 60 μm, the cellular optical texture ended abruptly and no detectable birefringence was noted in the fibroin. In contrast, in the major ampullate silk duct of the *Nephila* spider the silk protein shows birefringence with a positive sign for some distance after the end of cellular optical texture[35] before the birefringence finally disappears some distance before the start of the draw down taper.[38] This suggests that there may be some difference in the behavior of the fibroin in the two organisms. However, the eventual loss of birefringence in both cases may result from the disruption of wall anchoring of the molecules as the linear velocity of the fibroin increases as a consequence of the continued convergence of the duct. The lack of birefringence persisted in the silkworm duct until the point at which the fibroin and surrounding thin layer of sericin suddenly pulled away from the cuticle lining of the duct in an internal draw down taper (see Figure 4a). This occurred between 4 and 0.6 mm from the start of the silk press in different individuals, the variation in the position probably depending on variations in the spinning conditions. Figure 4b shows that the specific retardance of the nascent fibroin brin increased rapidly, nearly reaching an asymptote within 500 μm. The increase in specific retardance was approximately inversely proportional to the declining thickness of the fibroin brin (graph not shown). The increase in specific retardance is likely to result from an increase in molecular alignment produced by extensional flow of the partially gelled fibroin in the draw down taper. The specific retardance of the brins after they had emerged from the spigot was appreciably higher than the asymptotic value seen in the nascent silk at the distal end of the duct, indicating that more orientation is introduced later in the secretory pathway (see below). An internal draw down is also seen in an analogous location in the duct in whole mounts of orb web spider silk glands[39] and shows a similar asymptotic increase in specific retardation with distance (James Higham, unpublished results). The sericin formed a continuous thin nonbirefringent layer surrounding the fibroin up to the start of the internal draw down taper, but thereafter in the gland duct the sericin layer broke up into a series of large irregular blobs coating the fibroin, suggesting that it remained fluid.

Structure of the Silk Press. Figure 5 shows micrographs of selected cross-sections of the silk press and related structures, while Figure 6 shows the three-dimensional reconstruction obtained from serial sections. The distal ends of the two silk gland ducts join to give a common duct 150 μm long with a wide lumen which in turn opens into the lumen of the silk press. The nascent silk brins have evidently already drawn down before reaching the common duct (Figure 4a). This confirms our observation above and those of Magoshi of internal draw down processing in the duct.[4] The cuticle lining of the silk press is much thickened and is lip-shaped in the transverse section. Its lumen is much flattened dorsoventrally and bow-shaped. The shape of the lumen appears to be partly defined by two stiff plates in the cuticle lining close to the edge of the lumen: a large ventral plate (approximately 70 μm in length) and a much narrower but much longer dorsal plate. The start of both dorsal and ventral plates and the finish of the dorsal plate define the length (300 μm) of the silk press proper. The plates did not cut well and are therefore probably quite hard. Left and right dorsal and smaller left and right ventral muscles (arrows in Figure 5d,e)

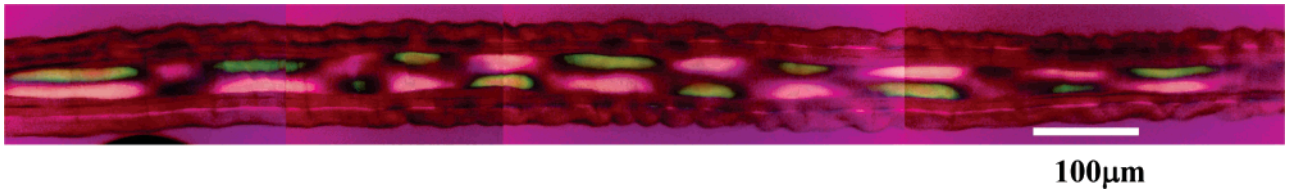

Figure 3. A montage of polarizing micrographs showing the cellular optical texture (see the text) in the fibroin in situ within the duct. The slow axis of the polarizer was at 45° to the long axis of the duct, and a first-order red compensator was used. In life the fibroin flowed from left to right along the duct. The scale bar equals 100 μm.

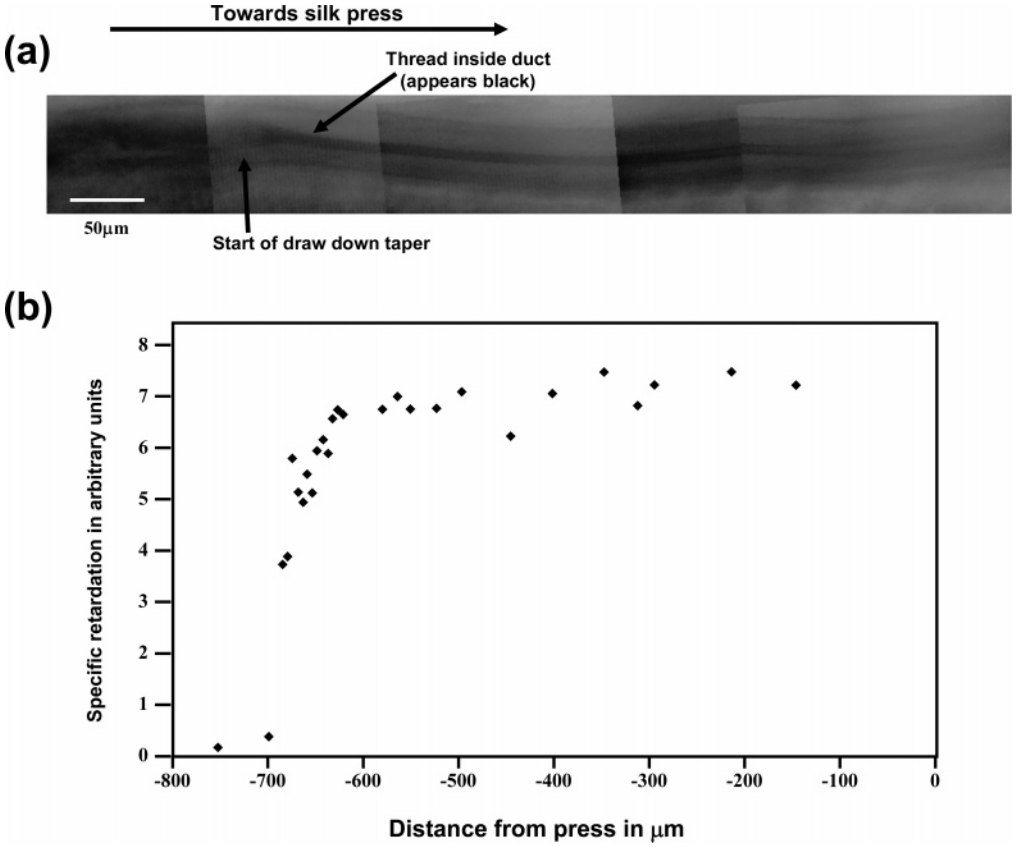

Figure 4. Changes in birefringence in the internal draw down taper within the distal part of the spinning duct. (a) Montage of photomicrographs of a whole mount of the duct taken with crossed polars and an λ4 compensator showing the increase in birefringence (appears black at the arrow) in the fibroin in the internal draw down taper. The slow axis of the polarizer was maintained at 45° to the long axis of the duct. (b) Changes in the specific retardance at different distances along the duct. Note that the *x* axes of (a) and (b) are aligned at the start of the draw down taper but have different horizontal scales.

have their origins dorsally and laterally, respectively, on the cuticle surrounding the lumen of the silk press and run more or less radially with respect to the lumen of the silk press to insert onto the cuticle of the head capsule. This pattern of origin and insertion and the radial orientation of the muscles strongly indicate that their contraction would separate the dorsal and ventral plates, increasing the diameter and volume of the lumen of the silk press. Flexible cuticle at the corners of the lip-shaped cuticle may act as spring-loaded hinges, allowing the press to return to the substantially closed position when the muscles relax. The lumen between the stiff plates appears to form the fibroin filaments (see Figure 5g,h) into a cross-sectional shape similar to that of the fully formed brins. The fluid sericin is evidently able to pass through the lumen on either side of the fibroin filaments where the latter are squeezed between the stiff plates. This is thought to be facilitated by the bow shape of the lumen.

After the silk press, the lumen runs for 470 μm in the spinning duct, becoming approximately circular in cross-section before opening at the tip of the spigot from which the bave emerges to the outside world. Figure 7 shows changes in the cross-sectional area of the lumen as it travels through the silk press and related structures. The cross-sectional area of the lumen markedly diminished at the start of the silk press, and this constriction was maintained until the lumen finally dilated in the last part of the spinning duct before it opened at the spigot.

In our previous paper[26] we used molecular dynamics calculations on poly(Ala-Gly), a model of the crystalline domain of *B. mori* silk fibroin, to simulate the conversion from a silk I state before spinning to the silk II state found in the fully formed silk fiber. Removal of the water shell surrounding the predominantly hydrophobic fibroin molecules (hydrophobic dehydration) in the last stage of the simulation had the effect of reproducing the transformation from silk I to the heterogeneous silk II structure as monitored by changes in peptide backbone torsion angles. This suggests that water removal produced by a combination of wall shear and extensional flow as the nascent silk is drawn down into a filament is the predominant factor in inducing the conformation transition in in vivo spinning. Further, we suggest that the constriction of the lumen between the stiff

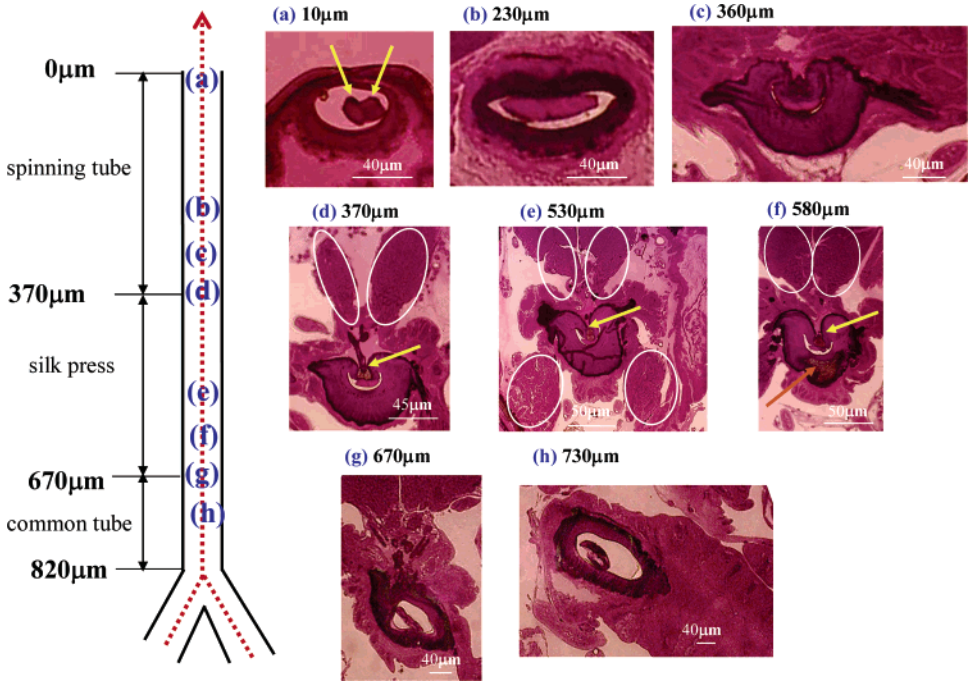

Figure 5. Optical micrographs of the cross-section of a spinneret. (a) Near the spigot of the silkworm. There is a pair of fibroin filaments (arrows) in the elliptical lumen. (b) The lumen becomes flatter. (c) The lumen becomes bow-shaped, and the wall of the spinneret becomes fatter. (d) There is a narrow plate (arrow) above the lumen. The two dorsal muscles are shown (elipses). (e) The two dorsal and two ventral muscles can be seen from here to 580 μm inward from the spigot. (f) Two muscles below the lumen disappear, and a plate appears below the lumen. (g, h) At 670 μm inward from the spigot, the shape of the lumen changes dramatically.

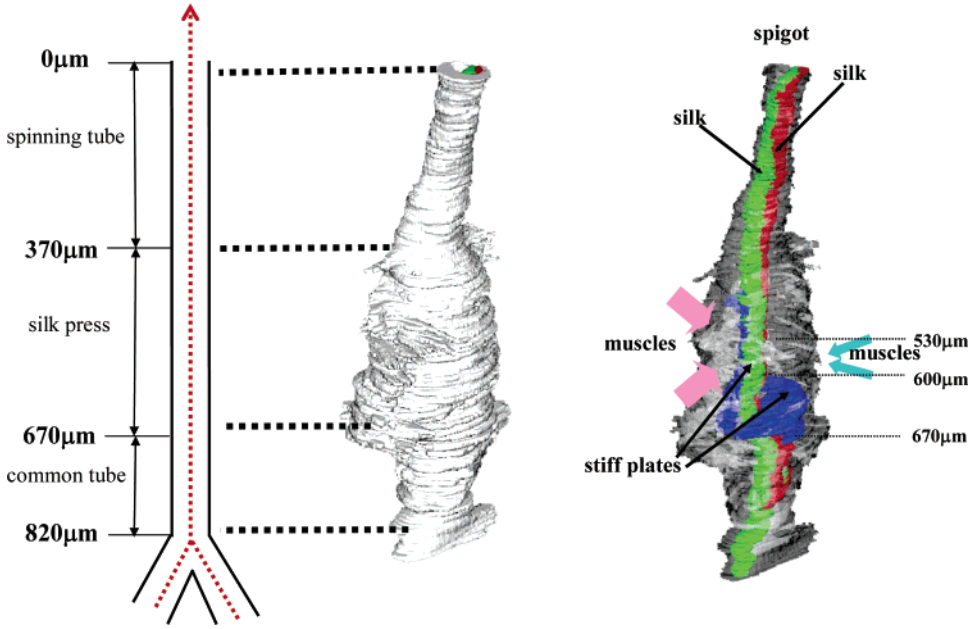

Figure 6. Three-dimensional reconstruction of the spinneret showing a pair of silk threads (red and green) and the stiff plates (purple). The reconstruction was performed from about 1000 optical micrographs of transverse sections of a silk press and related structures using the software TRI/3D-VOL (RATOC System Engineering Co. Ltd., Tokyo). Pink and light blue arrows indicate the muscles (Figure 5e).

plates of the silk press can play a part in spinning by acting as an elongated constriction die to induce shear and/or extensional flow. This is borne out by the observation that birefringence of the nascent brin increased markedly within the filter press during artificial drawing of silk from the spigot at low speeds,[16,21] indicating an alignment of the fibroin molecules produced by wall shear and/or extensional flow. The elongation of the constriction die may lengthen the time that the nascent silk brin is exposed to mechanical forces and therefore produce a more complete conversion to the silk II state than could be achieved by a short constriction.

Further, the structure of the silk press suggests that the silkworm can actively regulate the cross-sectional area of the lumen under muscular control. Contraction of the dorsal and ventral muscles is thought to dilate the press, while their relaxation, together with the elastic recoil of the cuticle lining and pressure in the body cavity, is thought to allow the press to constrict again to its resting state. Active control of the silk

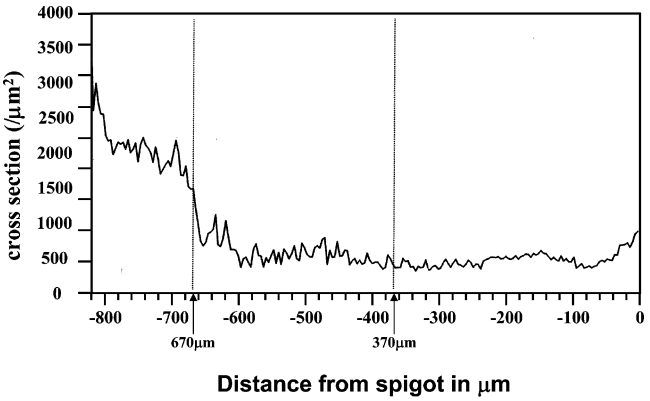

Figure 7. Changes in the cross-sectional area of the lumen as it passess through the silk press and related structures.

press is supported by two observations from Katoaka's work, although these are not cited as evidence for active control in the original papers:[16,21] (i) fast artificial reeling caused the marked increase in birefringence of the fibroin to occur in the gland duct rather than in the silk press probably as a result of dilation of the silk press; (ii) treatment with ether caused the marked increase of birefringence to occur within the silk press rather than the gland duct probably as a result of relaxation of the dorsal and ventral muscles and consequent constriction of the silk press. Our results do not rule out the possibility that the silk press, like the valve, a somewhat similar structure at the posterior end of the duct in the major ampullate gland of spiders,[39] may additionally act as a micropump for silk fibroin under certain circumstances. Our observations also support the hypothesis that the silk press and, as in spiders,[32,35,40] the internal draw down in the distal part of the duct both facilitate the conversion of silk I to silk II. Thus, evidence that postdrawing dramatically improves the tensile strength in fibers extruded artificially from solutions of regenerated *B. mori* fibroin[41] suggests a parallel with our observations on the natural spinning mechanism. Our observations and hypothesis for the function of the silk duct and silk press in spinning are summarized in Figure 8.

In conclusion, our observations contribute to a further understanding of the natural spinning process in silkworms and highlight its similarity to that used by spiders to make tough dragline silk. In addition, they may facilitate the development of biomimetic industrial spinning methods. Finally, we suggest that hydrophobic dehydration produced by the strain or shear of both extracellular and intracellular protein gels may represent a smart, adaptive mechanism for controlling protein polymerization widespread throughout the animal kingdom and used for the assembly of the fibrous proteins of silks, related materials, and connective tissue proteins. Such a mechanism would be smart and adaptive in that it would produce fibers in the right place and with the right orientation to oppose applied stresses. Our observations also suggest that the linear secretory

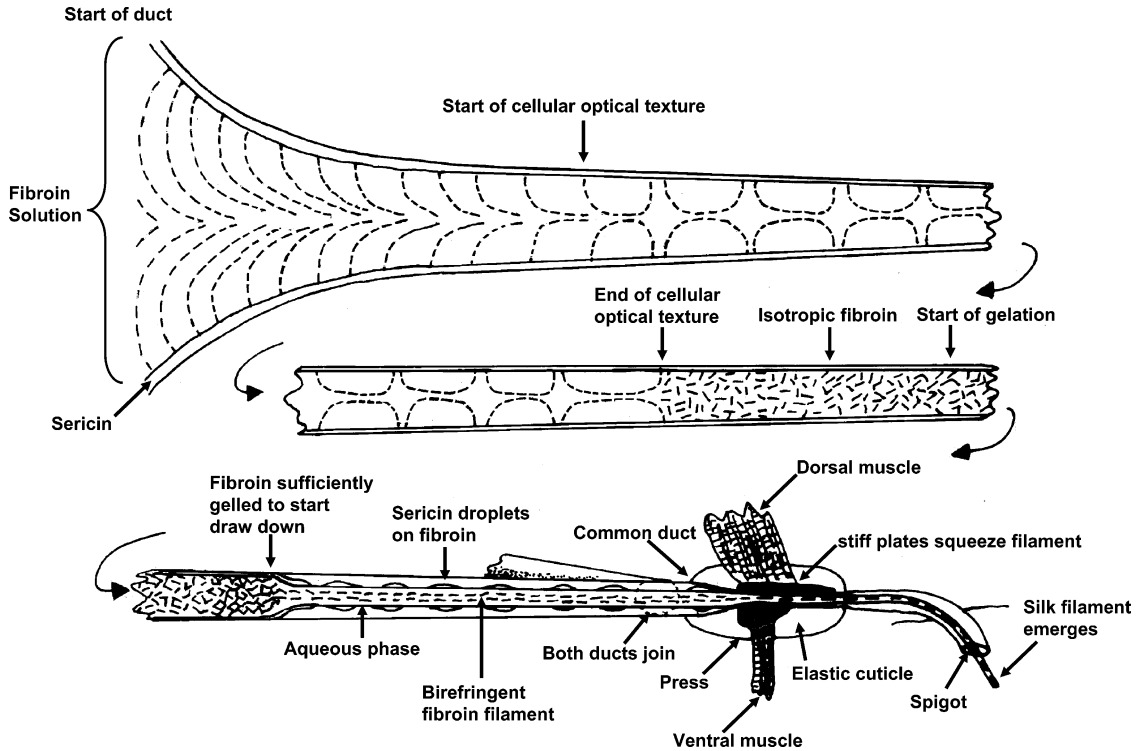

Figure 8. Diagram showing a lateral view of the silk duct and silk press summarizing our observations and hypothesis for the function of these structures in silk spinning. Fibroin enters the duct from the anterior part of the silk gland as a highly viscous liquid crystalline sol. The curved lines indicate the molecular director of the rod-shaped fibroin molecules. Tapering of the silk duct induces the cellular optical texture at a critical lumen diameter. Further down the duct, this optical texture disappears abruptly at a critical linear velocity at which shear at the fibroin/sericin interface just overcomes anchoring of the fibroin molecules. Secretion of hydrogen ions into the lumen of the spinning duct by the proton pump in the cells lining the duct produces a downward pH gradient in the duct. The reduction in pH suppresses the negative charge in the aspartic and glutamic acid residues in heavy-chain fibroin inducing a weak gelling of the fibroin. Changes in the interactions between heavy-chain fibroin, light-chain fibroin, and P25[42] may also play a role in the dope processing and gelation. This increase in viscosity induces a transition from Couette flow to rapid extensional flow, inducing an internal draw down taper. The rapid extensional flow produced in this way orientates the fibroin molecules and draws them together, initiating the removal of the water shell around the hydrophobic fibroin and hence initiating silk II formation. The nascent fibroin filament then enters the constriction between the stiff plates of the silk press, which acts as a restriction die. This results in further extensional flow, water removal, and molecular orientation, leading to further formation of silk II.

pathway of silk-secreting arthropods provides an excellent model system for studying this phenomenon.

Acknowledgment. We acknowledge support from the Insect Technology Project, Japan, and the Agriculture Biotechnology Project, Japan. T.A. thanks Dr. Kozo Tsubouchi (Kataoka) for many useful discussions. D.K. acknowledges support from the U.K. Engineering and Physical Science and Biotechnology and Biological Research Councils. D.K. thanks Prof. Fritz Vollrath for use of his laboratory and help and support in many ways.

References and Notes

(1) Asakura, T.; Kaplan, D. L. Silk Production and Processing. In *Encyclopedia of Agricultural Science*; Arutzen, C. J., Ed.; Academic Press: New York, 1994; Vol. 4, pp 1−11.
(2) Shao, Z.; Vollrath, F. *Nature* **2002**, *418*, 741.
(3) Altman, G.; Horan, R.; Lu, H.; Moreau, J.; Martin, I.; Richmond, J.; Kaplan, D. *Biomaterials* **2002**, *23*, 4131−4141.
(4) Magoshi, J.; Magoshi, Y.; Nakamura, S. *ACS Symp. Ser.* **1994**, *544*, 292−310.
(5) Magoshi, J.; Magoshi, Y.; Nakamura, S. *Polym. Commun.* **1985**, *26*, 309−11.
(6) Magoshi, J.; Magoshi, Y.; Nakamura, S. *Sen'i Gakkaishi* **1997**, *53*, P87−P97.
(7) Azuma, M.; Ohta, Y. *J. Exp. Biol.* **1998**, *201*, 479−486.
(8) Zhou, L.; Chen, X.; Shao, Z.; Huang, Y.; Knight, D. P. *J. Phys. Chem. B* **2005**, *109*, 16937−16945.
(9) Terry, A. E.; Knight, D. P.; Porter, D.; Vollrath, F. *Biomacromolecules* **2004**, *5*, 768−772.
(10) Foo, C. W. P.; Bini, E.; Hensman, J.; Knight, D. P.; Lewis, R. V.; Kaplan, D. L. *Appl. Phys. A: Mater. Sci. Process.* **2006**, *82*, 223−233.
(11) P.H. Sericulture, http://www.tnau.ac.in/notesbscag/ser, 2003.
(12) Horard, B.; Julien, E.; Nony, P.; Garel, A. *Mol. Cell. Biol.* **1997**, *17*, 1572−1579.
(13) Grzelak, K. *Comp. Biochem. Physiol., B: Biochem. Mol. Biol.* **1995**, *110*, 671−681.
(14) Inoue, S.; Tanaka, K.; Tanaka, H.; Ohtomo, K.; Kanda, T.; Imamura, M.; Quan, G. X.; Kojima, K.; Yamashita, T.; Nakajima, T.; Taira, H.; Tamura, T.; Mizuno, S. *Eur. J. Biochem.* **2004**, *271*, 356−366.
(15) Matsunami, K.; Kokubo, H.; Ohno, K.; Suzuki, Y. *Dev., Growth Differ.* **1998**, *40*, 591−597.
(16) . Kataoka, K. *Sen'i Gakkaishi* **1978**, *34*, 80−88.
(17) Garel, A.; Deleage, G.; Prudhomme, J. C. *Insect Biochem. Mol. Biol.* **1997**, *27*, 469−477.
(18) Sorensen, G. S.; Cribb, B. W.; Merritt, D.; Johnson, M. L.; Zalucki, M. P. *Arthropod Struct. Dev.* **2006**, *35*, 3−13.
(19) Ogiwara, S. In *Anatomy of spinneret and the mechanism of fiber formation of B. mori silkworms;* Ito, T., Ed.; Kensi-no-Kouzou; Chi Kumakai Publishing Co.: Ueda, Japan, 1957; pp 20−45.
(20) Kataoka, K.; Umatsu, I. *Koubunnshi Ronbunsyu* **1977**, *34*, 37−41.
(21) Kataoka, K.; Umatsu, I. *Koubunnshi Ronbunsyu* **1977**, *34*, 457−464.
(22) Asakura, T.; Ashida, J.; Yamane, T.; Kameda, T.; Nakazawa, Y.; Ohgo, K.; Komatsu, K. *J. Mol. Biol.* **2001**, *306*, 291−305.
(23) Asakura, T.; Ohgo, K.; Komatsu, K.; Kanenari, M.; Okuyama, K. *Macromolecules* **2005**, *38*, 7397−7403.
(24) Asakura, T.; Yao, J.; Yamane, T.; Umemura, K.; Ulrich, A. S. *J. Am. Chem. Soc.* **2002**, *124*, 8794−8795.
(25) Asakura, T.; Yao, J. *Protein Sci.* **2002**, *11*, 2706−2713.
(26) Yamane, T.; Umemura, K.; Nakazawa, Y.; Asakura, T. *Macromolecules* **2003**, *36*, 6766−6772.
(27) Akai, H. *Experientia* **1983**, *39*, 443−449.
(28) Maser, M. D.; Powell, T. E., 3rd; Philpott, C. W. *Stain Technol.* **1967**, *42*, 175−182.
(29) Greenwalt, T. J.; Domino, M. M.; Dumaswala, U. J. *Vox Sang.* **1992**, *63*, 272−275.
(30) Nicolson, G. L.; Marchesi, V. T.; Singer, S. J. *J. Cell Biol.* **1971**, *51*, 265−272.
(31) Knight, D. P.; Feng, D.; Stewart, M. *Biol. Rev. Cambridge Philos. Soc.* **1996**, *71*, 81−111.
(32) Knight, D. P.; Vollrath, F. *Biomacromolecules* **2001**, *2*, 323−334.
(33) Neville, A. C.; Luke, B. M. *J. Cell Sci.* **1971**, *8*, 93−109.
(34) McClung, C. *McClung's Handbook of Microscopical Technique, the microscopical investigation of biological materials with polarized light microscopy*, 3rd ed.; Cassel & Co.: London, 1950; p 421.
(35) Knight, D. P.; Vollrath, F. *Proc. R. Soc. London, B* **1999**, *266*, 519−523.
(36) Ochi, A.; Hossain, K. S.; Magoshi, J.; Nemoto, N. *Biomacromolecules* **2002**, *3*, 1187−1196.
(37) Bunning, J. D.; Lydon, J. E. *Liq. Cryst.* **1996**, *20*, 381−385.
(38) Knight, D. P.; Vollrath, F. *Philos. Trans. R. Soc. London, B: Biol. Sci.* **2002**, *357*, 155−163.
(39) Vollrath, F.; Knight, D. P. *Int. J. Biol. Macromol.* **1999**, *24*, 243−249.
(40) Knight, D. P.; Knight, M. M.; Vollrath, F. *Int. J. Biol. Macromol.* **2000**, *27*, 205−210.
(41) Ha, S. W.; Tonelli, A. E.; Hudson, S. M. *Biomacromolecules* **2005**, *6*, 1722−1731.
(42) Foo, C. W. P.; Bini, E.; Hensman, J.; Knight, D. P.; Lewis, R. V.; Kaplan, D. L. *Appl. Phys. A: Mater. Sci. Process.* **2006**, *82*, 223−233.

BM060874Z